quantum reports

MDPI

Perspective

From Integer Quantized Hall Plateaus to Z_2 Topological Surfaces: Quantum Capacitance as a Probe of the Boundary Density of States

Afif Siddiki

Vocational School, Atlas University, Anadolu Str. 40, 34408 Istanbul, Türkiye; afif.siddiki@atlas.edu.tr

Abstract

The integer quantum Hall effect (IQHE), Z_2 topological insulators (TIs), and quantum capacitance are generally treated as separate subjects, yet they share a common thread: bulk topology gives rise to a protected boundary state, and quantum capacitance is one of the few electrostatic methods able to detect the density of states (DOS). This paper examines that connection, restricted to single-particle band topology; the fractional QHE is a many-body phase outside this scope, treated separately. The IQHE showed that quantized boundary transport has a topological (Chern-number) origin, a result later extended to zero field in Z_2 insulators with helical edge and Dirac surface states. Quantum capacitance has become a key technique for mapping the Landau-level bulk DOS underlying the QHE and the boundary Dirac DOS of topological surfaces. Self-consistent screening theory complicates this: the bulk divides into compressible and incompressible regions that shift with the magnetic field, and local impedance measurements read as quantum capacitance show the bulk is not uniformly incompressible even while the plateau remains quantized. This paper argues that quantum capacitance is one of the clearest windows into the boundary DOS that topology imposes—while remaining insensitive to the invariant itself—and reveals the local, field-dependent character of the 'insulating bulk' assumption behind the QHE–TI analogy.

Keywords: quantum Hall effect; topological insulators; quantum capacitance; density of states; incompressible strips; Landau levels; Dirac surface states

1. Introduction

The quantum Hall effect (QHE), topological insulators (TIs), and quantum capacitance are generally presented in textbooks as three distinct topics—the quantum Hall effect as a transport phenomenon, topological insulators as a class of materials, and quantum capacitance as a device-physics concept. In reality, however, they are closely related. The QHE was the first experimental example in which a bulk topological invariant controlled a measurable, quantized physical quantity [1–3]. Topological insulators extended this concept to zero magnetic field by employing spin–orbit coupling in place of a Landau-quantizing field to generate topologically protected boundary states [4–9]. Although quantum capacitance is not a topological quantity by itself, it is one of the very few electrostatic quantities that are directly sensitive to the density of states (DOS) resulting from these topological band structures—which makes it a suitable diagnostic tool for both types of systems.

The claim made here is deliberately bounded. Quantum capacitance is not a measurement of topology: neither the Chern number nor the Z_2 index can be extracted from a

Check for updates

Academic Editor: Michel Planat

Received: 9 August 2026
Revised: 30 August 2026
Accepted: 30 August 2026
Published: 31 August 2026

Copyright: © 2026 by the author. Licensee MDPI, Basel, Switzerland. This article is an open access article distributed under the terms and conditions of the Creative Commons Attribution (CC BY) license.

compressibility measurement. What quantum capacitance probes is the density of states that a given invariant enforces at the boundary—and it does so across systems that are otherwise studied with entirely different techniques. That is the sense in which it is described here as unifying, and the distinction is developed in Section 3 and revisited in Section 7.

2. The Quantum Hall Effect and Its Topological Origin

Von Klitzing, Dorda, and Pepper found that the Hall resistance of a two-dimensional electron gas (2DEG) in a strong perpendicular magnetic field shows plateaus at the values $h/\nu e^2$, where the integer ν is the filling factor, and that these values are independent of the sample's geometry or degree of disorder [1]. Two years later, Tsui, Störmer, and Gossard observed additional plateaus at fractional filling factors in higher-mobility samples at lower temperature—the fractional quantum Hall effect, which arises from a correlated electron liquid rather than from any splitting of the integer plateaus [2]. The fractional effect is a many-body phase and lies outside the scope of the present discussion; the reasons are set out in Section 7.

The integer quantum Hall plateaus were later understood not as an accident of a particular material but as a consequence of a topological invariant—the first Chern number, or TKNN invariant, of the filled Landau-level bands [3]. Each filled, non-degenerate Landau level contributes exactly one quantum of Hall conductance—two, where spin degeneracy is unresolved—and for that number to change, the bulk energy gap would have to close. The robustness of the plateaus against disorder is thus a manifestation of topological robustness and not of the material's purity; Laughlin's gauge argument had already established this robustness on general grounds, without reference to a specific band structure [10]. The insight that a bulk topological index determines the number of protected, dissipationless edge channels is the conceptual basis on which the field of topological insulators was built, and the transport consequences of those channels were formalized in the multiprobe scattering picture of Landauer and Büttiker [11].

This statement requires one refinement that matters for what follows. In a disordered sample the Landau levels are broadened into bands in which only states near the center are extended, the remainder being localized by the random potential [12,13]. The quantized value of σ_{xy} is protected as long as no extended states lie at the Fermi energy—that is, by a mobility gap rather than a spectral gap. The distinction is not a technicality. Localized states are what give the plateaus their finite width, since they absorb the change in carrier density as the field is swept and pin E_F between Landau-level centers; a disorder-free system would show quantization only at isolated fields. They also carry thermodynamic weight: $\partial n/\partial \mu$ does not vanish when E_F lies among them. Exact quantization of the Hall resistance is therefore compatible with a bulk of finite thermodynamic density of states, and the two should not be conflated [12–15].

3. From Landau Levels to Topological Insulators

The natural question was whether a similar bulk–boundary correspondence could arise in the absence of an external magnetic field. Kane and Mele demonstrated theoretically that spin–orbit coupling in systems similar to graphene could lead to a "quantum spin Hall" state: a time-reversal-symmetric version of the quantum Hall effect in which electrons with spin up and those with spin down travel in opposite directions along the edge, the state being protected by a Z_2 topological invariant rather than a Chern number [4]. Bernevig, Hughes, and Zhang then predicted that HgTe/CdTe quantum wells could realize this state [5], a prediction that König et al. confirmed experimentally through quantized edge conduction [6].

The idea soon extended to three dimensions. Zhang et al. predicted that Bi_2Se_3, Bi_2Te_3, and Sb_2Te_3 host a single gapless Dirac cone in spin–momentum-locked surface states that wrap an insulating bulk, and Y. Xia et al. confirmed this by angle-resolved photoemission spectroscopy (ARPES) [7,8]. The Colloquium by Hasan and Kane, along with the complementary review by Qi and Zhang, established the general classification of these phases and their connection to the integer QHE, describing the 2D topological insulator as "a close cousin of the integer quantum Hall state" and the 3D case as one that exhibits a topological magnetoelectric response [9,16].

The main point is this: in the quantum Hall effect a bulk Chern number determines the boundary conductance, whereas in topological insulators time-reversal-symmetric spin–orbit coupling produces a similar zero-field boundary state governed by a Z_2 invariant. In both cases the system has a gapped bulk and a metallic boundary. The two systems are not, however, symmetric in what a capacitance measurement can reach, and it is worth being explicit about this before the analogy is pushed further. The quantum Hall system is a two-dimensional bulk with a one-dimensional boundary: the chiral edge channels occupy a line at the sample perimeter and contribute negligibly to the capacitance of a gated Hall bar, so a capacitance measurement on a 2DEG reads the bulk spectrum—the Landau levels—and not the protected edge states themselves. A three-dimensional topological insulator inverts this: the bulk is nominally gapped and inert, while the protected Dirac state occupies the entire gated surface, so the same measurement reads the boundary. The Landau-level density of states and the Dirac surface density of states are therefore not two instances of the same object. The former is the bulk-gap signature of the quantum Hall system, and the latter the boundary signature of the topological insulator (Figure 1).

What is common is the role played by the density of states rather than the location at which it is measured. In each system the topology fixes a gapped bulk and a protected boundary, and quantum capacitance reads out whichever member of that pair is electrostatically accessible in the given geometry. In the quantum Hall case, that is the bulk: the vanishing density of states when E_F lies in a cyclotron gap is precisely the condition under which the Chern number is well defined and the plateau is quantized, so the Landau-level oscillation is a thermodynamic verification of the gap that guarantees the edge channels, observed in place of the channels themselves. In the topological insulator case, it is the boundary: the linear Dirac density of states is the state that the bulk Z_2 index guarantees, measured directly. Figure 1 and Table 1 set out the correspondence; Figure 2 shows the three density-of-states profiles that follow from it. The one case in which this geometric restriction has been partly overcome is discussed in Section 6, where contacts placed inside the Hall bar give the capacitance measurement spatial resolution within the quantum Hall bulk itself.

Table 1. Bulk and boundary density-of-states signatures in the two systems, and which of them reaches a quantum-capacitance measurement in each case. The asymmetry in the last row is geometric rather than conceptual: the quantum Hall boundary is one-dimensional and occupies a negligible fraction of the gated area, whereas the topological-insulator boundary is two-dimensional and occupies all of it.

	Quantum Hall Effect (2DEG)	**Three-Dimensional Topological Insulator**
Invariant	Chern number (TKNN)	Z_2 index
Bulk	Two-dimensional; Landau-quantized, gapped when E_F lies in a cyclotron gap	Three-dimensional; band-gapped

Table 1. *Cont.*

	Quantum Hall Effect (2DEG)	**Three-Dimensional Topological Insulator**
Bulk DOS signature	Landau-level oscillations; DOS suppressed but not zero within the mobility gap (localized states)	DOS $\to 0$ within the band gap (ideal case)
Boundary	One-dimensional chiral edge channels	Two-dimensional Dirac surface state
Boundary DOS signature	Edge-channel DOS; negligible gated area	Linear Dirac DOS, $c_Q \propto \lvert \varepsilon_F \rvert$
What c_Q measures in practice	The bulk: Landau levels [17]; locally resolved within the bulk [18]	The boundary: Dirac surface state [19,20]

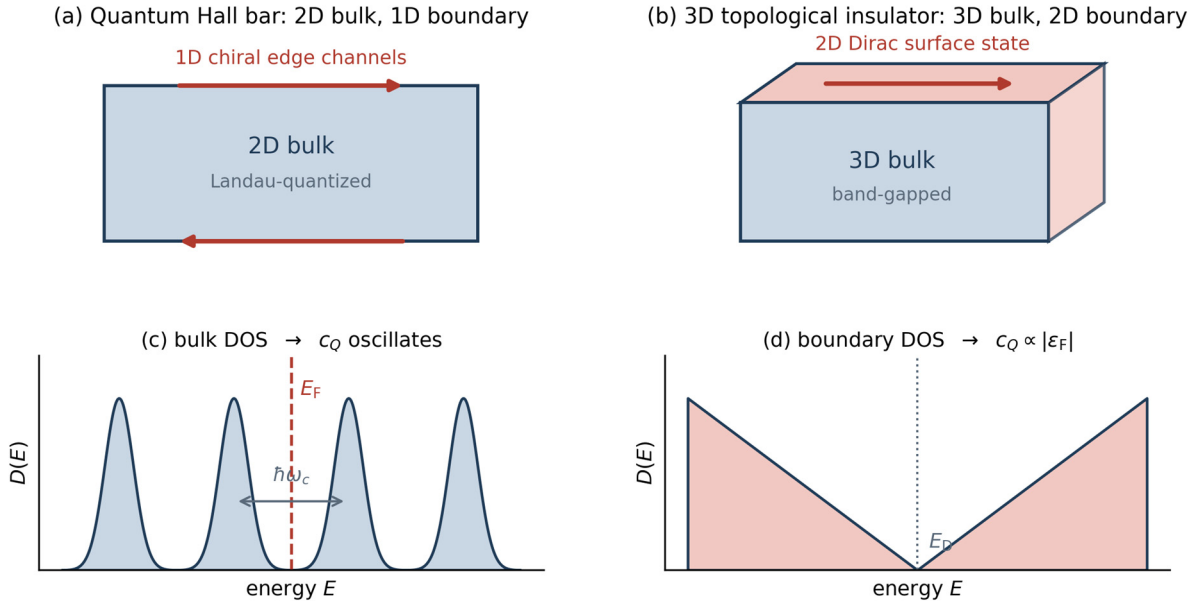


Figure 1. The bulk–boundary structure of the two systems and the density of states a capacitance measurement reaches in each. (**a**) A quantum Hall bar is a two-dimensional bulk with a one-dimensional boundary: the chiral edge channels run along the perimeter and occupy a negligible fraction of the gated area, so the measurement reads the bulk. (**b**) A three-dimensional topological insulator inverts the arrangement: the bulk is band-gapped and the protected Dirac state occupies the entire surface, so the measurement reads the boundary. (**c**) The corresponding bulk density of states in the quantum Hall case, with E_F lying in a cyclotron gap, so that c_Q oscillates as the field is swept. (**d**) The boundary density of states of the topological insulator, linear in energy about the Dirac point E_D, giving $c_Q \propto \lvert \varepsilon_F \rvert$. Panels (**a**,**b**) are schematic; no scale is implied. Colors are used consistently throughout: blue denotes the gapped bulk and its density of states, and red the topologically protected boundary and its density of states. The red arrows in (**a**,**b**) mark the propagation direction of the protected boundary state, counter-propagating along the two edges of the Hall bar in (**a**) and running over the whole surface in (**b**). In (**c**) the dashed red line marks the Fermi energy and the double-headed arrow the cyclotron gap; in (**d**) the dotted line marks the Dirac point.

It is worth being specific here about what quantum capacitance, the thermodynamic quantity $c_Q = e^2(\partial n/\partial \mu)$ formally introduced in Section 4, does and does not do. A topological invariant, like the Chern number for the quantum Hall effect or the Z_2 index for a topological insulator, is an integer that is a globally defined property of the filled bulk band structure. It is quantized, cannot change by smooth deformations of the Hamiltonian, and can only change if a bulk gap closes. It is not itself an observable quantity in the

thermodynamic sense: the Chern number is not directly measured, but rather deduced from the number and chirality of the protected boundary channels it guarantees. Quantum capacitance, in contrast, continuously probes the density of states at the Fermi level as a function of energy. In a bulk gap, the presence of the invariant is reflected in the density of states only indirectly, through the existence and dispersion of the boundary states that the gap protects, and through the vanishing (or finite) density of states in the bulk itself. Thus, the measured density of states profile is a reflection of the underlying topology, not the invariant itself, and one should not treat the two as if the quantum capacitance were "measuring" the topological number.

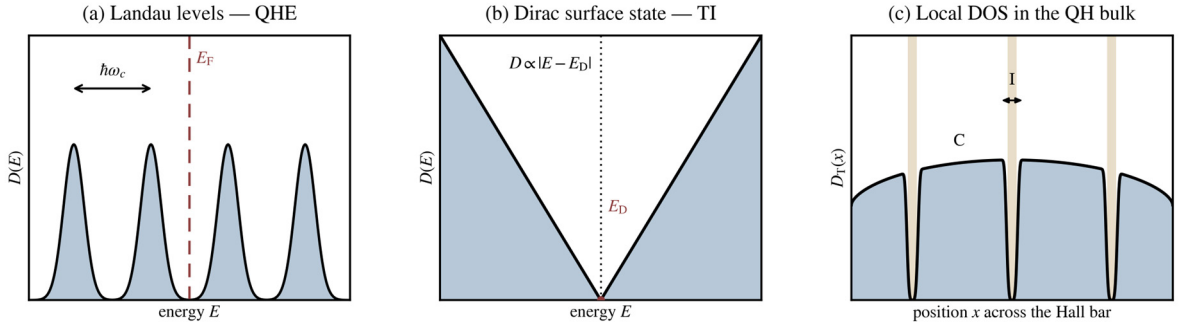


Figure 2. The three density-of-states profiles at issue. (**a**) In the quantum Hall effect, the bulk DOS collapses into broadened, macroscopically degenerate Landau levels separated by cyclotron gaps, so the quantum capacitance oscillates as E_F is swept through them. (**b**) The topological surface state of a three-dimensional TI has a linear Dirac DOS vanishing at E_D, giving $c_Q \propto |\varepsilon_F|$. Panels (**a**,**b**) are functions of energy and refer to the idealized, translationally invariant bulk that the topological classification describes. (**c**) The same quantity resolved in real space across an actual Hall bar: self-consistent screening splits the sample into compressible regions (C) with a finite thermodynamic DOS and incompressible strips (I, shaded) with $D_T = 0$ and therefore zero quantum capacitance, whose widths and positions move continuously with magnetic field while the global topological index and the quantized plateau stay fixed. Axes are schematic; no scale is implied. The color coding is the same throughout: the blue area under each curve is the density of states itself, the vertical tan bands in (**c**) mark the incompressible strips (I), and the unshaded regions between them the compressible regions (C); the dashed red line in (**a**) marks the Fermi energy and the dotted line in (**b**) the Dirac point.

4. Quantum Capacitance as a Probe of the Density of States

Luryi showed that a two-dimensional electron system does not behave as an ideal metallic capacitor plate, because its density of states is finite and it therefore screens the applied field only partially. This adds a further (quantum) capacitance in series with the geometric one, $c_Q = e^2(\partial n/\partial \mu)$, which is proportional to the density of states at the Fermi level (E_F) [21]. Here n is the areal carrier density, so that c_Q is a capacitance per unit area; the quantum capacitance of a region of area A is $C_Q = c_Q A$. Lower-case c_Q is used throughout for the intensive quantity and upper-case C_Q where the capacitance of a specific region or device is meant. Unlike transport measurements, which depend on scattering and mobility, quantum capacitance is a thermodynamic, near-equilibrium measurement: it directly indicates compressibility and the density of states, even in samples so disordered that clean transport is not possible.

In graphene and in other two-dimensional electron gases, this method reveals the density of states with great clarity—for example, J. Xia et al. employed quantum capacitance to map the density of states of graphene, resolving both its linear dependence on energy and its finite residual value at the Dirac point [22]. When a magnetic field is applied, the quantum capacitance oscillates in step with the discrete density of states of the Landau

levels, providing an independent thermodynamic check of the Landau quantization responsible for the quantum Hall effect and complementing measurements of Hall-plateau transport [17].

5. Quantum Capacitance of Topological Surface States

The same reasoning holds for TI surface states. Since the topological surface state has a linear Dirac dispersion, its density of states is zero at the Dirac point and increases linearly with $|E - E_D|$, which results in $c_Q \propto |\varepsilon_F|$, as opposed to the constant density of states (and therefore constant c_Q) found in a conventional 2DEG. Experiments carried out on Bi_2Se_3 have exploited precisely this feature: RF quantum-capacitance measurements allowed the Dirac velocity of the topological surface state to be obtained directly from the slope of c_Q with respect to gate voltage by means of the Berglund integral—the standard capacitance–voltage inversion of metal–oxide–semiconductor analysis—without requiring prior knowledge of the band structure [19]. Other capacitance studies have used the excitation-frequency dependence of c_Q to distinguish the surface response from that of the bulk in thin-film Bi_2Se_3 capacitors [20], while theoretical work on ultrathin films has traced how Zeeman coupling and inter-surface hybridization govern the crossover between coupled and decoupled top and bottom Dirac surfaces [23].

The relation $c_Q \propto |\varepsilon_F|$ is an idealization, and real devices depart from it in several ways that matter when it is used quantitatively. Charge inhomogeneity broadens the Dirac point into a distribution of local potentials, so the density of states does not reach zero and the measured capacitance saturates at a finite minimum rather than closing to a cusp; the same effect is familiar in graphene, where a finite residual capacitance at the Dirac point is routinely observed [22]. Finite temperature acts similarly, since the measurement averages the density of states over a window of order k_BT about the Fermi level, and the depth of the minimum is set by whichever of disorder broadening and thermal broadening is larger. Residual bulk carriers are a further complication: as-grown Bi_2Se_3 is typically n-type, and bulk states then contribute a capacitance in parallel with the surface term, so that reaching the bulk-depleted regime, or separating the two by their different response times, is a precondition for reading the slope as a surface property [19,20]. Both surfaces of a slab contribute in parallel, and in thin films they hybridize, which modifies the spectrum further [23]. Finally, gating does not shift the Fermi level rigidly. Band bending near the gated surface can populate trivial two-dimensional accumulation-layer subbands whose density of states adds to the Dirac term, and the conversion from gate voltage to E_F through the Berglund integral is only as reliable as the assumption that the measured capacitance belongs to the surface state alone. None of this invalidates the method, but it does mean that an approximately linear c_Q is a necessary rather than a sufficient indication of a Dirac surface state, a point returned to in Section 7.

In the presence of an applied magnetic field, the TI surface states also give rise to Landau levels, and their quantum capacitance exhibits the same oscillatory pattern as that observed in ordinary 2DEGs and in graphene, although the oscillations are predicted to be asymmetrically centered on the Dirac point and to scale with the square root of the field rather than with the field itself, which would be a direct thermodynamic signature of the relativistic Dirac Landau-level spectrum [23]. This completes the experimental parallel—though at the level of the density of states, not of the invariant: quantum capacitance, which was first developed for conventional 2DEGs [21] and employed to verify the Landau-level density of states associated with the QHE, is now a standard electrostatic method for characterizing the Dirac surface states that make topological insulators the zero-field analogs of the QHE [9]. What such a measurement establishes, however, is the form of the density of states and not the topology. A linear, Dirac-like density of states is consistent

with a topologically protected surface state, but it does not by itself fix the Z_2 invariant, and an unprotected Dirac cone would produce the same signature; the point is taken up again in Section 7.

6. Local Compressibility and the Limits of the Bulk-Insulator Picture

Before turning to the electrostatic picture, it is worth distinguishing the sense of "bulk" used in Section 3 from the one used below. The topological classification is a statement about the global bulk: it concerns the filled bands of an idealized, translationally invariant system, and the invariant it defines takes a single value for the sample as a whole. Local incompressibility, by contrast, is a statement about the real, finite, electrostatically inhomogeneous sample: it describes how the density of states and screening response vary from point to point across the Hall bar, and it can change continuously with magnetic field and position even while the global topological index stays fixed. A locally compressible region within the bulk is therefore not a violation, or even a complication, of the bulk topological gap in the idealized sense—it reflects the fact that a real device is not translationally invariant and must be treated electrostatically. The two descriptions operate at different levels: one classifies the system as a whole, the other maps its local thermodynamic response, and quantum capacitance is sensitive only to the latter.

One further distinction should be made explicit, since the terminology invites conflation. Compressibility, $\partial n/\partial \mu$, is a thermodynamic quantity: it measures how the electron density responds to a change in chemical potential. Conductivity is a transport quantity: it measures how current responds to an applied field. A region of finite $\partial n/\partial \mu$ need not conduct—disorder-localized states are compressible and insulating at the same time—and a region of vanishing $\partial n/\partial \mu$ is not thereby shown to block current along every path. The words compressible and incompressible are used in this section in the thermodynamic sense only, and carry no implication about dc transport. Quantum capacitance measures the former and says nothing directly about the latter.

The picture presented in Section 3—a gapped, incompressible bulk with protected conducting boundaries—rests on a single-particle approximation. Building on the electrostatic picture of edge channels introduced by Chklovskii, Shklovskii and Glazman [24], Siddiki and Gerhardts devised a self-consistent screening theory of the integer quantum Hall effect that treats the two-dimensional electron system electrostatically at finite temperature. Solving the Thomas–Fermi–Poisson equation for the density profile shows that a Hall bar separates into locally compressible regions (which have a finite thermodynamic density of states) and locally incompressible strips (which have vanishing density of states and are pinned to an integer Landau-level filling) whose width and position change continuously as the magnetic field changes [25]. In this model the plateau is sustained by an incompressible strip wide enough to suppress backscattering between the edges of the sample, and not by the bulk being incompressible everywhere; the extremely narrow strips predicted by the simple Thomas–Fermi approximation are broadened once the finite spatial extent of the electron wavefunctions and the effects of nonlocal transport are taken into account [25].

It is worth stating plainly how this description relates to the conventional one, since the two are sometimes presented as competitors. They are better understood as answering different questions. The topological argument of Section 2 explains why the plateau value is exactly $h/\nu e^2$ and why it is insensitive to sample details; it is formulated for an idealized, translationally invariant, non-interacting system. The disorder–localization picture explains why the plateaus have finite width in magnetic field, since localized states absorb the change in carrier density and pin E_F between Landau-level centers [12–15]; it is a single-particle account in which disorder is the essential ingredient. The self-consistent screening picture addresses a third question—where the current flows and how the density

of states is distributed in space—and it is an interacting, electrostatic, finite-temperature account in which the confining potential and the Coulomb interaction are essential. None of these supersedes the others, and a real sample contains both localized states and a self-consistently screened density profile. Their relative importance is a matter of sample quality: disorder-dominated, low-mobility samples are the natural domain of the localization description, whereas high-mobility samples, in which comparatively few localized states are available to pin the Fermi energy across a wide plateau, are better described by the electrostatic structure. The measurements discussed below were made on high-mobility GaAs/AlGaAs material, which is why the screening picture is emphasized here; this is a statement about the regime under discussion and not a claim that the localization picture is incorrect.

A finite bulk thermodynamic density of states across a plateau therefore admits more than one origin, and it is worth separating them. Disorder-localized states contribute $\partial n/\partial \mu$ throughout the mobility gap, as described in Section 2. Self-consistent screening contributes a spatially structured density of states, with compressible regions of finite $\partial n/\partial \mu$ separated by incompressible strips whose width and position track the magnetic field. Thermal broadening contributes a third. These are not alternatives, and no capacitance measurement separates them by itself: quantum capacitance responds to $\partial n/\partial \mu$ and is indifferent to whether the states it counts are localized or extended. What distinguishes the screening contribution is not its magnitude but its structure in field and position. Localization produces a smooth background that varies slowly across a plateau, whereas the compressible–incompressible pattern produces a signal keyed to where the incompressible strip lies relative to the contacts, and therefore a non-monotonic dependence within a single plateau.

This picture yields a directly testable prediction, framed in the same physical quantity introduced in Section 4: since incompressible regions have a zero thermodynamic density of states, they should also have zero quantum capacitance, $C_Q = c_Q A = e^2 D_T(E_F) A$, where $D_T(E_F) = \partial n/\partial \mu$ is the thermodynamic density of states at the Fermi energy—the same quantity introduced in Section 4—and A is the relevant area. Local probes had already shown that the quantum Hall bulk is not homogeneous: single-electron-transistor measurements of the local compressibility resolved the coexistence of compressible and incompressible regions and the way localized states rearrange across a plateau [26]. Kendirlik et al. then probed this directly inside the bulk, inserting two further voltage probes into a high-mobility GaAs/AlGaAs Hall bar and measuring the local AC impedance between them while the outer contacts simultaneously recorded the usual, fully quantized Hall plateau [18]. The quantity actually measured is a complex impedance at finite excitation frequency, not a capacitance read off a gated parallel-plate structure. Quantum capacitance enters at the level of interpretation: the reactive part of the inner-contact response is attributed to the thermodynamic density of states of the region between the probes, on the argument that an incompressible region with $D_T(E_F) = 0$ would present zero capacitance and hence a diverging impedance. If the bulk were uniformly incompressible, as is assumed in the simplest single-particle bulk-topological argument, the inner impedance should therefore have diverged throughout the entire plateau. Instead, the measured inner potential difference—and therefore the local quantum capacitance inferred from it—remained finite throughout, peaking only in a narrow subsection of each plateau ($\nu = 2$ and 1, and also at $\nu = 2/3$, for which see the caveat in Section 7) and falling away elsewhere within the same plateau, thus clearly showing that the bulk is compressible over a large part of the field range in which the Hall resistance is already perfectly quantized [18]. When the temperature was raised, the maximum value decreased in proportion to the inverse of the thermodynamic density of states, which is what the quantum-capacitance interpretation

predicts and an unrelated cross-coupling would not; this supports that interpretation, but the density of states remains an inference from the impedance data rather than a directly recorded capacitance. This does not exclude a localized-state contribution to the measured density of states, and none is claimed to be excluded: the feature relevant here is the variation across the plateau rather than the finite value itself.

The outcome is in agreement with, not a refutation of, the QHE–TI analogy presented in Section 3: the Hall plateau still arises from the presence of incompressible strips, and therefore from a nonzero energy gap along some path that either spans or goes around the sample, this being consistent with a nonzero Chern number [18,25]. The local measurement complicates the assumption of an everywhere incompressible bulk that underlies the most straightforward formulations of the bulk-boundary correspondence: in actual devices the boundary between "protected edge and insulating bulk" [11] is not sharp but is instead determined self-consistently by electrostatics, screening, and the local filling factor. This provides a second, independent example of the diagnostic capability of quantum capacitance beyond the topological-insulator surface states discussed in Section 5: just as the same $c_Q = e^2(\partial n/\partial \mu)$ relationship shows the presence of a Dirac surface DOS in a TI, it also shows that the "bulk-insulator" part of the structural analogy between the QHE and the TI is a local and field-dependent statement rather than a literal one [18,25].

Independent support for this picture has since come from systems in which the same question can be asked at zero magnetic field. In magnetically doped topological insulators exhibiting the quantum anomalous Hall effect, potentials measured at multiple points within a device are well described by assuming current flow through the two-dimensional bulk rather than along edge modes [27], and scanning-SQUID magnetic imaging of the current density has directly visualized a regime in which the sample carries current primarily in its interior [28]. The imaging work concludes further that the current flows through incompressible regions whose spatial structure changes as the plateau is traversed, and that the self-consistent electrostatics of the sample play a central role in setting the current distribution. These are magnetometry and transport experiments rather than capacitance measurements, and they address the zero-field rather than the field-induced case, so they do not test the argument made here directly. They do indicate, however, that the departure from a uniformly incompressible, edge-only picture is not peculiar to the high-mobility GaAs system discussed above, and that it appears on the topological-insulator side of the analogy as well.

A further, more strongly interacting instance of spatial inhomogeneity lies within reach of the same local-probe strategy. In the second and higher Landau levels, Coulomb interactions among the electrons of the partially filled level favor charge-density-wave ground states—unidirectional stripe phases near half filling, and triangular "bubble" phases (clusters of electrons arranged on a Wigner-crystal-like lattice) near quarter and three-quarter filling—rather than the liquid-like states familiar from the lowest Landau level [29]. These phases were first inferred from a strongly anisotropic longitudinal resistance near half filling of the topmost Landau level [30], and the bubble phases are associated with reentrant integer quantum Hall states (RIQHE), in which the Hall resistance returns to a quantized plateau over a filling-factor range flanked by non-quantized, compressible behavior on either side [31]. Because these are collective, interaction-driven charge patterns rather than either single-particle disorder or the self-consistent, non-interacting screening profile discussed above, they lie outside the single-particle topological framework of Sections 2 and 3 in the same sense developed in Section Scope: Single-Particle Band Topology and the Fractional Regime; the reentrant plateaus they produce are not organized by the Chern number of a filled band but, if the cyclotron-braid classification of interacting two-dimensional systems is invoked, by the commensurability-based invariants that classify multi-particle

correlated phases more generally [32]. A locally resolved compressibility measurement—of the kind used above to map $\partial n/\partial \mu$ across a Hall bar—is in principle well suited to distinguishing a spatially uniform incompressible strip from the periodic or textured compressible–incompressible pattern that a stripe or bubble phase would produce, and could therefore offer direct, spatially resolved evidence for the charge ordering that the RIQHE is believed to reflect, complementing the anisotropic-transport evidence obtained so far. To my knowledge, this specific comparison has not yet been carried out; I note it here as a natural extension of the local-probe approach reviewed in this paper rather than as an established result.

7. What Quantum Capacitance Cannot Do

The most fundamental limitation is one of principle, and it was set out in Section 3: quantum capacitance returns a thermodynamic quantity evaluated locally and at the Fermi level, not a topological invariant. It is worth adding what follows from this. The density-of-states features discussed above—the discrete Landau-level spectrum, the linear Dirac DOS of a protected surface state, the vanishing DOS of an incompressible region—are necessary signatures of the corresponding topological phases, but they are not sufficient ones. A linear density of states is equally consistent with an unprotected Dirac cone, and a locally vanishing density of states with trivial localization. Establishing that a boundary state is topologically protected still requires spin-resolved photoemission, quantized transport, or band-structure classification; quantum capacitance is complementary to those methods rather than a replacement for them.

Advocating quantum capacitance as a probe requires being explicit about where it is weak. The measured device capacitance is the geometric capacitance in series with the quantum capacitance, so extracting a density of states demands independent knowledge of the gate geometry and the dielectric constant; the two contributions are hardest to separate precisely where the quantum capacitance is small—near the Dirac point, and inside an incompressible region—which are exactly the regimes of interest here. Parasitic capacitance, series resistance, and charge trapping at interfaces distort the measured response at high frequency, and the finite charging time of a poorly conducting sample can mimic a vanishing density of states. The measurement also averages over the electrode area, so a local statement about compressibility is only as local as the contact geometry permits: the inner-contact arrangement of Ref. [18] pushes that spatial resolution into the bulk, but it is not a microscope, and there the density of states is extracted from an impedance rather than read from a gated capacitor, so the frequency and series-resistance caveats above bear directly on its interpretation. Quantum capacitance is also blind to localization. It counts states at the Fermi level without regard to whether they conduct, so a finite c_Q does not by itself imply a conducting bulk, and a transport measurement showing $\sigma_{xx} \to 0$ is not in tension with a capacitance measurement showing $\partial n/\partial \mu \neq 0$ at the same field. Statements about compressibility and statements about conduction are separate, and this probe speaks only to the former. None of this undermines the argument above. It sets out the conditions under which the measured capacitance can be read as a density of states rather than as a device response.

Scope: Single-Particle Band Topology and the Fractional Regime

A final limitation is one of scope, and it is worth stating explicitly. The topological classification used throughout this paper is that of single-particle band topology: the Chern number of filled Landau-level bands in the integer quantum Hall effect, and the Z_2 index of a time-reversal-symmetric band insulator. Both are properties of the occupied bands of an effectively non-interacting system, and both are what the density-of-states signatures

discussed here reflect. The fractional quantum Hall effect is not of this kind. It is an intrinsically many-body phase whose ground state is a correlated liquid, whose gap is a many-body gap rather than a cyclotron or band gap, and whose elementary excitations carry fractional charge and obey non-trivial exchange statistics [33]. It cannot be reached from the statement that each filled Landau level contributes one conductance quantum, and the arguments of Sections 2 and 3 should not be read as covering it.

Several frameworks describe the fractional regime, and they differ in construction rather than in their predictions for the observed fillings. The Laughlin wave function is a variational ansatz for the many-body ground state, built from lowest-Landau-level orbitals and Jastrow-type correlations [33]. The composite-fermion construction instead attaches an even number of flux quanta to each electron and maps the fractional problem onto an effective integer quantum Hall effect of composite fermions [34]. Chern–Simons field theory recasts the same flux attachment as an effective gauge theory at the level of an action rather than a wavefunction. The homotopy-based, cyclotron-braid alternative starts from a different primitive still: it restricts the exchange trajectories accessible to the particles in the magnetic-field-constrained multiparticle configuration space, selects the braid subgroups compatible with that restriction, and recovers Laughlin–Jastrow correlations and a wider hierarchy from the selected subgroups [32,35,36]. In this framework the classifying invariant is not a Chern number but a cyclotron-braid commensurability condition between the classical cyclotron orbit and the electron separation set by the classical Wigner lattice, and the homotopy classes of multi-particle braids selected by this condition have been proposed to correspond, essentially one-to-one, to the observed hierarchy of FQHE filling fractions [32]. This distinction is worth stating plainly against the single-particle invariants of Sections 2 and 3: the Chern number and the Z_2 index discussed there are properties of the filled bands of an effectively non-interacting system, whereas the commensurability invariant just described classifies an interacting, multi-particle correlated state and has no single-particle analog—the two should not be conflated when the word "topological" is applied to the IQHE and the FQHE in the same breath. The four constructions converge closely on which fillings are allowed and on the existence of a many-body gap; they differ in what is taken as fundamental—a variational wavefunction, a mean-field flux attachment, an effective action, or a restricted braid group—and a systematic comparison of what each predicts beyond the filling sequence itself (edge structure, non-Abelian generalizations, and so on) is beyond the scope of the present Perspective. I note these approaches without adjudicating between them, since none of them is what quantum capacitance is being used to probe here.

It is worth placing these constructions within a single classification, since the field-driven and zero-field cases are sometimes discussed as if the pairing were only IQHE–TI. Single-particle band topology in fact comes in two field/zero-field pairs. One pair carries a Chern number and requires broken time-reversal symmetry: the IQHE (Section 2), realized with an external magnetic field, and the quantum anomalous Hall effect or Chern insulator, its zero-field counterpart realized through magnetic doping or intrinsic magnetism and already encountered in Section 6 [27,28]. The other pair carries a Z_2 index and requires time-reversal symmetry, which forces the Chern number itself to vanish: this is the topological-insulator family of Section 3, which has no field-driven analogue for the same symmetry reason. The many-body counterparts follow the same field/zero-field split. The FQHE (Section 2 and above in this section) is the field-driven, many-body phase; fractional Chern insulators (FCIs) are its zero-field, lattice analog—a partially filled, topologically nontrivial (Chern-number-carrying) band stabilized by strong interactions rather than by an external field. FCIs share the correlated, many-body character of the FQHE rather than the single-particle band topology on which Sections 2 and 3 rest, so the scope restriction stated above

for the FQHE applies to them for the same reason. What is worth noting is that FCIs have been established in exactly the thermodynamic quantity this paper is about: local electronic compressibility measurements in magic-angle twisted bilayer graphene have resolved a sequence of incompressible states at fractional filling of a Chern band, each associated with a many-body gap analogous to the FQHE gap [37]. As with the $\nu = 1/3$ GaAs measurement discussed above, such a measurement establishes the magnitude of a compressibility gap, not the Chern number of the parent band or the statistics of the excitations it hosts; the distinction between a thermodynamic signature and a topological invariant that organizes this entire paper therefore extends, essentially unchanged, to the fractional Chern regime.

This bears directly on one point in Section 6. The inner-contact measurements were reported at $\nu = 2$ and $\nu = 1$ and also at $\nu = 2/3$, and the self-consistent screening analysis applied to them is a single-particle Thomas–Fermi treatment. Extending that analysis to a fractional filling is not automatic: it requires the composite-fermion mapping, under which the fractional state of electrons becomes an integer state of composite fermions and an analogous compressible–incompressible structure can be defined [34]. I therefore restrict the interpretation offered in Section 6 to the integer fillings, and record the $\nu = 2/3$ observation without claiming that the strip picture as presented accounts for it.

It should not be concluded that quantum capacitance has nothing to say about fractional phases. Compressibility is well defined in a correlated liquid, and capacitive measurements have been used to extract the chemical-potential discontinuity across a fractional gap, giving a thermodynamic measure of the many-body gap itself—for instance at $\nu = 1/3$ in GaAs [38]. What such a measurement returns is the magnitude of an incompressibility, not the statistics of the quasiparticles that produce it. Fractional charge and exchange statistics require interferometry, shot noise, or tunneling spectroscopy, and no thermodynamic compressibility measurement substitutes for them. The same distinction between a density of states and an invariant that is drawn in Section 3 for the integer case applies here and, if anything, more sharply.

8. Conclusions

The quantum Hall effect and topological insulators represent, respectively, the field-driven and zero-field routes to the same underlying principle: a bulk topological invariant enforces a protected, gapless boundary state with a characteristic density of states. Quantum capacitance, though originally introduced as a device-physics correction to ordinary parallel-plate capacitance in 2DEGs [21], is well suited to reading out this DOS structure, because it is a near-equilibrium electrostatic measurement rather than a transport measurement. In the QHE, quantum capacitance oscillations confirm the discrete, macroscopically degenerate Landau-level bulk DOS that underlies the quantized Hall plateaus [17]. In topological insulators, quantum capacitance measurements have directly extracted the Dirac velocity and mapped the linear boundary DOS associated with protected surface states, and have been used to disentangle bulk, depletion, and surface contributions in real devices [19,20]. Pushed further, local impedance measurements inside the quantum Hall bulk itself, read in terms of quantum capacitance, show that the textbook picture of a spatially uniform incompressible bulk is an idealization: self-consistent screening produces a patchwork of compressible and incompressible regions that rearranges with magnetic field even while the Hall plateau stays exactly quantized [18,25]—a description that complements, rather than replaces, the conventional disorder–localization account of plateau formation [12–15]. The broader lesson is that experimentally verifying a topological phase requires probes attuned to what topology actually constrains, and quantum capacitance, precisely because it measures compressibility rather than conductance, has become one of the most direct such probes, both across the field-induced and zero-field families

of topological matter and within the bulk of the quantum Hall system itself. Topology constrains the existence and protection of the boundary states; quantum capacitance probes the associated density of states, that is, the compressibility.

Funding: This research received no external funding.

Data Availability Statement: No new data were created or analyzed in this study. Data sharing is not applicable to this article.

Acknowledgments: I sincerely thank my PhD supervisor, the late Rolf R. Gerhardts, for all his contributions to screening theory.

Conflicts of Interest: The author declares no conflicts of interest.

References

1. von Klitzing, K.; Dorda, G.; Pepper, M. New Method for High-Accuracy Determination of the Fine-Structure Constant Based on Quantized Hall Resistance. *Phys. Rev. Lett.* **1980**, *45*, 494–497. [CrossRef]
2. Tsui, D.C.; Störmer, H.L.; Gossard, A.C. Two-Dimensional Magnetotransport in the Extreme Quantum Limit. *Phys. Rev. Lett.* **1982**, *48*, 1559–1562. [CrossRef]
3. Thouless, D.J.; Kohmoto, M.; Nightingale, M.P.; den Nijs, M. Quantized Hall Conductance in a Two-Dimensional Periodic Potential. *Phys. Rev. Lett.* **1982**, *49*, 405–408. [CrossRef]
4. Kane, C.L.; Mele, E.J. Z2 Topological Order and the Quantum Spin Hall Effect. *Phys. Rev. Lett.* **2005**, *95*, 146802. [CrossRef] [PubMed]
5. Bernevig, B.A.; Hughes, T.L.; Zhang, S.-C. Quantum Spin Hall Effect and Topological Phase Transition in HgTe Quantum Wells. *Science* **2006**, *314*, 1757–1761. [CrossRef] [PubMed]
6. König, M.; Wiedmann, S.; Brüne, C.; Roth, A.; Buhmann, H.; Molenkamp, L.W.; Qi, X.-L.; Zhang, S.-C. Quantum Spin Hall Insulator State in HgTe Quantum Wells. *Science* **2007**, *318*, 766–770. [CrossRef] [PubMed]
7. Zhang, H.; Liu, C.-X.; Qi, X.-L.; Dai, X.; Fang, Z.; Zhang, S.-C. Topological Insulators in Bi_2Se_3, Bi_2Te_3 and Sb_2Te_3 with a Single Dirac Cone on the Surface. *Nat. Phys.* **2009**, *5*, 438–442. [CrossRef]
8. Xia, Y.; Qian, D.; Hsieh, D.; Wray, L.; Pal, A.; Lin, H.; Bansil, A.; Grauer, D.; Hor, Y.S.; Cava, R.J.; et al. Observation of a Large-Gap Topological-Insulator Class with a Single Dirac Cone on the Surface. *Nat. Phys.* **2009**, *5*, 398–402. [CrossRef]
9. Hasan, M.Z.; Kane, C.L. Colloquium: Topological Insulators. *Rev. Mod. Phys.* **2010**, *82*, 3045–3067. [CrossRef]
10. Laughlin, R.B. Quantized Hall Conductivity in Two Dimensions. *Phys. Rev. B* **1981**, *23*, 5632–5633. [CrossRef]
11. Büttiker, M. Absence of Backscattering in the Quantum Hall Effect in Multiprobe Conductors. *Phys. Rev. B* **1988**, *38*, 9375–9389. [CrossRef] [PubMed]
12. Aoki, H.; Ando, T. Effect of Localization on the Hall Conductivity in the Two-Dimensional System in Strong Magnetic Fields. *Solid State Commun.* **1981**, *38*, 1079–1082. [CrossRef]
13. Prange, R.E. Quantized Hall Resistance and the Measurement of the Fine-Structure Constant. *Phys. Rev. B* **1981**, *23*, 4802–4805. [CrossRef]
14. Halperin, B.I. Quantized Hall Conductance, Current-Carrying Edge States, and the Existence of Extended States in a Two-Dimensional Disordered Potential. *Phys. Rev. B* **1982**, *25*, 2185–2190. [CrossRef]
15. Huckestein, B. Scaling Theory of the Integer Quantum Hall Effect. *Rev. Mod. Phys.* **1995**, *67*, 357–396. [CrossRef]
16. Qi, X.-L.; Zhang, S.-C. Topological Insulators and Superconductors. *Rev. Mod. Phys.* **2011**, *83*, 1057–1110. [CrossRef]
17. Smith, T.P.; Goldberg, B.B.; Stiles, P.J.; Heiblum, M. Direct Measurement of the Density of States of a Two-Dimensional Electron Gas. *Phys. Rev. B* **1985**, *32*, 2696–2699. [CrossRef] [PubMed]
18. Kendirlik, E.M.; Sirt, S.; Kalkan, S.B.; Ofek, N.; Umansky, V.; Siddiki, A. The Local Nature of Incompressibility of Quantum Hall Effect. *Nat. Commun.* **2017**, *8*, 14082. [CrossRef] [PubMed]
19. Inhofer, A.; Duffy, J.; Boukhicha, M.; Bocquillon, E.; Palomo, J.; Watanabe, K.; Taniguchi, T.; Estève, I.; Berroir, J.-M.; Fève, G.; et al. RF Quantum Capacitance of the Topological Insulator Bi2Se3 in the Bulk Depleted Regime for Field-Effect Transistors. *Phys. Rev. Appl.* **2018**, *9*, 024022. [CrossRef]
20. Xiu, F.; Meyer, N.; Kou, X.; He, L.; Lang, M.; Wang, Y.; Yu, X.; Fedorov, A.V.; Zou, J.; Wang, K.L. Quantum Capacitance in Topological Insulators. *Sci. Rep.* **2012**, *2*, 669. [CrossRef] [PubMed]
21. Luryi, S. Quantum Capacitance Devices. *Appl. Phys. Lett.* **1988**, *52*, 501–503. [CrossRef]
22. Xia, J.; Chen, F.; Li, J.; Tao, N. Measurement of the Quantum Capacitance of Graphene. *Nat. Nanotechnol.* **2009**, *4*, 505–509. [CrossRef] [PubMed]

23. Tahir, M.; Sabeeh, K.; Schwingenschlögl, U. Quantum Capacitance of an Ultrathin Topological Insulator Film in a Magnetic Field. *Sci. Rep.* **2013**, *3*, 1261. [CrossRef] [PubMed]
24. Chklovskii, D.B.; Shklovskii, B.I.; Glazman, L.I. Electrostatics of Edge Channels. *Phys. Rev. B* **1992**, *46*, 4026–4034. [CrossRef] [PubMed]
25. Siddiki, A.; Gerhardts, R.R. Incompressible Strips in Dissipative Hall Bars as Origin of Quantized Hall Plateaus. *Phys. Rev. B* **2004**, *70*, 195335. [CrossRef]
26. Ilani, S.; Martin, J.; Teitelbaum, E.; Smet, J.H.; Mahalu, D.; Umansky, V.; Yacoby, A. The Microscopic Nature of Localization in the Quantum Hall Effect. *Nature* **2004**, *427*, 328–332. [CrossRef] [PubMed]
27. Rosen, I.T.; Andersen, M.P.; Rodenbach, L.K.; Tai, L.; Zhang, P.; Wang, K.L.; Kastner, M.A.; Goldhaber-Gordon, D. Measured Potential Profile in a Quantum Anomalous Hall System Suggests Bulk-Dominated Current Flow. *Phys. Rev. Lett.* **2022**, *129*, 246602. [CrossRef] [PubMed]
28. Ferguson, G.M.; Xiao, R.; Richardella, A.R.; Low, D.; Samarth, N.; Nowack, K.C. Direct Visualization of Electronic Transport in a Quantum Anomalous Hall Insulator. *Nat. Mater.* **2023**, *22*, 1100–1105. [CrossRef] [PubMed]
29. Koulakov, A.A.; Fogler, M.M.; Shklovskii, B.I. Charge Density Wave in Two-Dimensional Electron Liquid in Weak Magnetic Field. *Phys. Rev. Lett.* **1996**, *76*, 499–502. [CrossRef] [PubMed]
30. Lilly, M.P.; Cooper, K.B.; Eisenstein, J.P.; Pfeiffer, L.N.; West, K.W. Evidence for an Anisotropic State of Two-Dimensional Electrons in High Landau Levels. *Phys. Rev. Lett.* **1999**, *82*, 394–397. [CrossRef]
31. Deng, N.; Kumar, A.; Manfra, M.J.; Pfeiffer, L.N.; West, K.W.; Csáthy, G.A. Collective Nature of the Reentrant Integer Quantum Hall States in the Second Landau Level. *Phys. Rev. Lett.* **2012**, *108*, 086803. [CrossRef] [PubMed]
32. Jacak, J.E. Topological Approach to Electron Correlations at Fractional Quantum Hall Effect. *Ann. Phys.* **2021**, *430*, 168493. [CrossRef]
33. Laughlin, R.B. Anomalous Quantum Hall Effect: An Incompressible Quantum Fluid with Fractionally Charged Excitations. *Phys. Rev. Lett.* **1983**, *50*, 1395–1398. [CrossRef]
34. Jain, J.K. *Composite Fermions*; Cambridge University Press: Cambridge, UK, 2007.
35. Jacak, J.E. Formal Derivation of the Laughlin Function and Its Generalization for Other Topological Phases of FQHE. *Sci. Rep.* **2022**, *12*, 616. [CrossRef] [PubMed]
36. Jacak, J.E. Forbidden Trajectories for Path Integrals. *Phys. Rev. A* **2023**, *107*, 032207. [CrossRef]
37. Xie, Y.; Pierce, A.T.; Park, J.M.; Parker, D.E.; Khalaf, E.; Ledwith, P.; Cao, Y.; Lee, S.H.; Chen, S.; Forrester, P.R.; et al. Fractional Chern Insulators in Magic-Angle Twisted Bilayer Graphene. *Nature* **2021**, *600*, 439–443. [CrossRef] [PubMed]
38. Eisenstein, J.P.; Pfeiffer, L.N.; West, K.W. Compressibility of the Two-Dimensional Electron Gas: Measurements of the Zero-Field Exchange Energy and Fractional Quantum Hall Gap. *Phys. Rev. B* **1994**, *50*, 1760–1778. [CrossRef] [PubMed]

Disclaimer/Publisher's Note: The statements, opinions and data contained in all publications are solely those of the individual author(s) and contributor(s) and not of MDPI and/or the editor(s). MDPI and/or the editor(s) disclaim responsibility for any injury to people or property resulting from any ideas, methods, instructions or products referred to in the content.